

Electrochemical properties of nickel hydroxide films deposited galvanostatically

S.-J. Kim^a, M.-K. Hong^b, B.C. Kim^c, J.-K. Chung^b, G.G. Wallace^d and S.-Y. Park^{a,b,*}

^aDepartment of Ceramic Engineering, Gangneung-Wonju National University Gangneung, 210-702, Korea

^bTechnology Innovation Center for Fine Ceramic, Gangneung-Wonju National University, Gangneung, 210-702, Korea

^cNatural Science Research Institute, Department of Chemistry, Dongguk University, Seoul, 100-715, Korea

^dARC Centre of Excellence for Electromaterials Science, Intelligent Polymer Research Institute, AIIIM Facility, Innovation Campus, University of Wollongong, Wollongong, NSW 2522, Australia

A high specific capacitance was obtained for Ni(OH)₂ galvanostatically deposited onto a stainless-steel foil. The structure and surface morphology of the Ni(OH)₂ were studied using X-ray diffraction(XRD) analysis and scanning electron microscopy(SEM). A loosely packed structure containing individual Ni(OH)₂ particles with an average size of 10-20 nm was obtained. The thickness of the deposit was several micro met. The capacitive characteristics of the Ni(OH)₂ electrodes were investigated using cyclic voltammetry(CV) in a 1 M KOH electrolyte solution. A maximum specific capacitance of 1233 F g⁻¹ was obtained for the Ni(OH)₂ electrode with a voltage range 0-0.5 V. The effect of deposition conditions, such as the current density, and 0.1M aqueous solution of Ni(NO₃)₂·6H₂O on the electrochemical capacitance of the deposited Ni(OH)₂ films are discussed in detail.

Key words: Nickel hydroxide films, Galvanostatic deposition, Redox capacitor, Electrochemical properties.

Introduction

Recently, electrochemical capacitors (ECs) have received a great deal of attention due to the high power density and longer life cycle attainable compared to secondary batteries. Electrochemical capacitors also exhibit a high energy density compared with the conventional electrical double-layer capacitors (EDLC) [1-3]. They have many practical applications such as auxiliary power sources in combination with fuel cells, batteries for hybrid electric vehicles, back up and pulse power sources for mobile electric devices, etc [4].

Electrochemical capacitors (ECs) based on hydrous ruthenium oxides exhibit much higher specific capacitance than conventional carbon materials with remarkably high specific capacitance values ranging from 658 to 760 F g⁻¹ (from a single electrode) [5-7]. However, the high cost of this noble metal material limits practical use. Therefore, much effort has been aimed at searching for alternative inexpensive electrode materials with good capacitive characteristics. Materials investigated include NiO [8, 9], CoO_x [10], MnO₂ [11], Ni(OH)₂ [12], and Co(OH)₂ [13]. Amongst these electrode materials, Ni(OH)₂ is considered to be the most promising for applications in energy/power storage devices, due to its low cost and well-defined electrochemical redox activity [14-18]. To date, only limited reports on the capacitive

behavior of Ni(OH)₂ have appeared [19, 20]. The use of electrochemical techniques to produce Ni(OH)₂ provides control over the structure and morphology of the films deposited [21, 22]. Tan et al. electrochemically deposited mesoporous Ni(OH)₂ films from dilute surfactant solutions using potentiostatic deposition [23].

Here we studied the electrochemical properties of Ni(OH)₂ films on stainless-steel(SS) foil using galvanostatic deposition at various current densities. The micro-structure as well as the electrochemical properties of the synthesized Ni(OH)₂ films were investigated.

Experimental

All chemical reagents were of analytical grade from Aldrich. A research grade stainless steel(SS) sheet (grade 304, t=0.2 mm) was used as the current collector. The stainless steel(SS) sheet was cut into the required size (10 mm × 30 mm). Stainless steel(SS) foil was polished with emery paper to a rough finish and then washed in acetone, ethyl alcohol and distilled water in turn for 10 minutes. A three-electrode electrochemical cell was assembled in which the stainless steel(SS) foil, platinum plate (20 mm × 20 mm) and a Ag/AgCl (in 1M KCl) were used as the working, counter and reference electrode, respectively. All electrochemical depositions of nickel hydroxide films were performed using a potentiostat (IM6 Instrument, Zanker electric, Germany).

Ni(OH)₂ was electrochemically deposited onto stainless steel(SS) foil in an electrolyte solution of 0.1M Ni(NO₃)₂·6H₂O under galvanostatic conditions. Galvanostatic deposition was carried out at various

*Corresponding author:
Tel : +82-33-655-2502
Fax: +82-33-655-2506
E-mail: sypark@gwnu.ac.kr

current densities. The deposited electrodes were washed in distilled water and then dried at room temperature for 24 h. The weight of the electrode was determined by means of a micro-balance. Deposited weight was calculated by weighing the substrate before and after deposition experiments, and after by drying at room temperature for 24 h.

The phase analysis of specimens was examined by X-ray diffraction (XRD) (D/MAX-2500 V, RIGAKU) with Cu K α radiation ($\lambda = 1.5406 \text{ \AA}$). The microstructures of the specimens were evaluated by field emission scanning electron microscopy (FE-SEM) (S-4700, HITACHI, Japan).

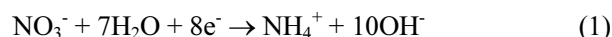
All electrochemical measurements were tested in a three-electrode arrangement. Cyclic voltammetry (CV) and electrochemical impedance spectroscopy (EIS) were carried out using an IM6 Instrument electrochemical work station (IM6ex, ZHNER Elektrik, Germany) at room temperature. The impedance measurements were conducted by means of an IM6 Instrument and an AC perturbation amplitude of 5 mV at 0.3 V was applied in the frequency range between 100 mHz and 100 kHz.

Results and Discussion

Fig. 1 shows the variation of the working electrode potential during galvanostatic deposition at various current densities. Galvanostatic depositions were performed in the range of 1-5 mA/cm². With current densities up to 4 mA/cm², the potential decreased with reaction time indicating deposition of a conductive layer on the electrode.

Corrigan and Bendert suggested that the electro-deposition of the Ni(OH)₂ films from the Ni(NO₃)₂ precursor involves the following steps [24]: Nitrate ions are reduced on the cathodic surface to produce hydroxide ions according to Equation (1).

The generation of OH⁻ at the cathode raises the local pH, resulting in the precipitation of α -Ni(OH)₂ at the electrode surface according to Equation (2):



Others[25] have shown that the predominant species present in concentrated Ni(NO₃)₂ aqueous solutions (ca. 1.8 M in our work) is the polymeric Ni₄(OH)₄⁴⁺. The polymeric species Ni₄(OH)₄⁴⁺ combines with OH⁻ to form a Ni(OH)₂ deposit as given in Equation (3):[26]



These reactions are likely to occur simultaneously during the electro-deposition process.

Fig. 2 shows the scanning electron microscope (SEM) images of the Ni(OH)₂ films formed at 3 mA/cm². As the current density increased, the deposited mass and area also increased. At higher magnification, deposited particles are shown to have agglomerated. The average diameter of nano-sized nickel hydroxide was 10 ~ 20 nm. It possesses a loosely packed structure, which is advantageous for the electrolyte ions to access the active materials for Faradaic reactions, and for the H⁺ or OH⁻ formed to migrate in time; which may contribute to an enhancement of capacitive performance.

Fig. 3 shows the X-ray diffraction (XRD) patterns of as-deposited nickel hydroxide before and after a cyclic voltammetry (CV) test. The diffraction pattern of as-

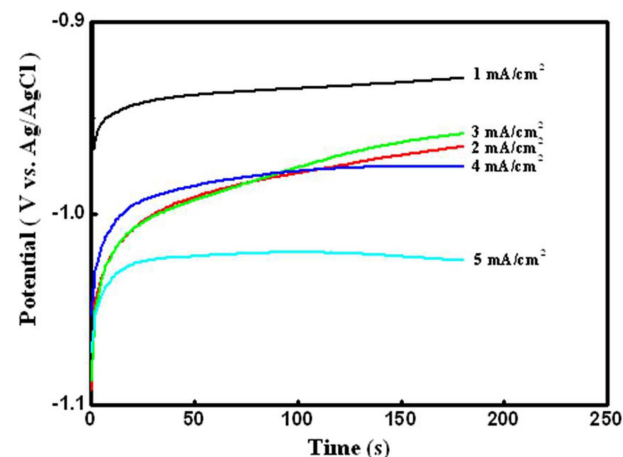


Fig. 1. Variation of the potential of the electrodes during galvanostatic deposition at different anodic current densities.

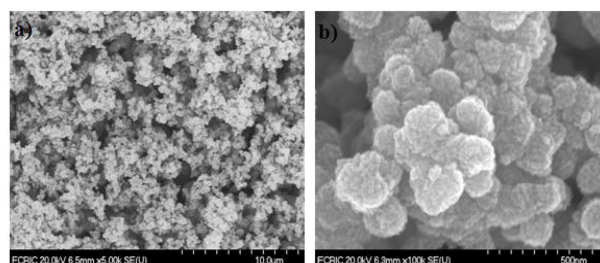


Fig. 2. Scanning electron microscope (SEM) images of Ni(OH)₂ electrodes prepared at a current density of (a) 3 mA/cm², (b) high magnification of (a).

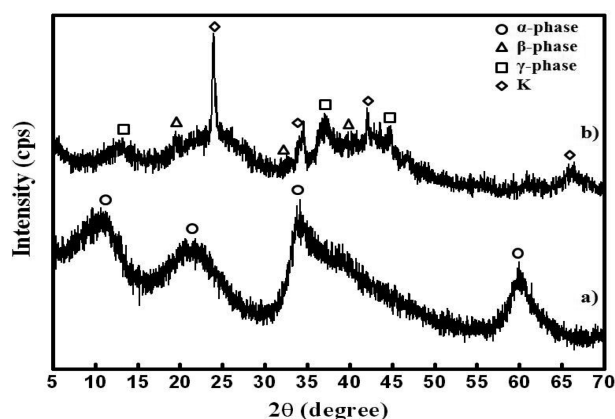


Fig. 3. X-Ray Diffraction (XRD) patterns of (a) before CV test, (b) after CV test of Ni(OH)₂.

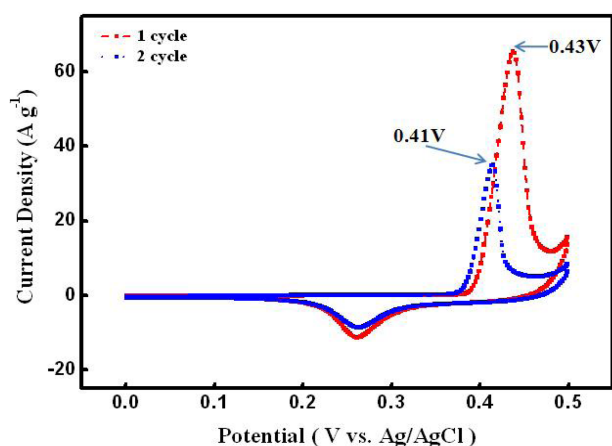


Fig. 4. Cyclic voltammograms(CV) of the Ni(OH)₂ electrodes prepared at a current density of 3 mA/cm².

deposited nickel hydroxide can be indexed to the diffraction data of the Ni(OH)₂ · 0.75H₂O (JCPDS No. 38-0715, rhombohedral) (Fig. 3 (a)). It can be assigned as the typical reflection of α-type Ni(OH)₂. However, after several cycles, γ-phase (JCPDS No. 84-1459, orthorhombic) and β-phase (JCPDS No. 74-2075, hexagonal) appeared (Fig.3 (b)). This implies that the surface state of the electrode would not return to its original state under the experimental conditions. It follows that the surface state of the electrode will hardly be restored to its original state as the cycle number increases. Also the X-ray diffraction(XRD) results shows that the crystallization of the γ-phase is induced by oxidation of Ni(OH)₂ to NiOOH for Ni.

Cyclic voltammetry(CV) is considered to be a suitable tool to indicate the capacitive behavior of any material. There is a pair of redox peaks, as a result of the Faradaic reaction of the Ni(OH)₂. For the Ni(OH)₂ electrode material, it is well known that the surface Faradaic reactions will proceed according to Equation (4)[27]:



The anodic peak is due to the oxidation of Ni(OH)₂ to NiOOH, and the cathodic peak is for the reverse process. One quasi-reversible electron transfer process is visible in the cyclic voltammetry(CV) curve, indicating that the measured capacitance is mainly based on a redox mechanism [28].

Cyclic voltammetry(CV) curves at a scan rate of 2 mVs⁻¹ for the nickel hydroxide electrode deposited at a 3 mA/cm² are presented in Fig. 4. One quasi-reversible electron transfer process was observed in the cyclic voltammetry(CV) curves, indicating that the measured capacitance is mainly based on a redox mechanism. The anodic peak is due to the oxidation of Ni(OH)₂ to NiOOH, and the cathodic peak is for the reverse process [29]. Cyclic voltammetry(CV) measurements show that the specific capacitance calculated from the first cyclic voltammetry(CV) curves was 2168 Fg⁻¹ and

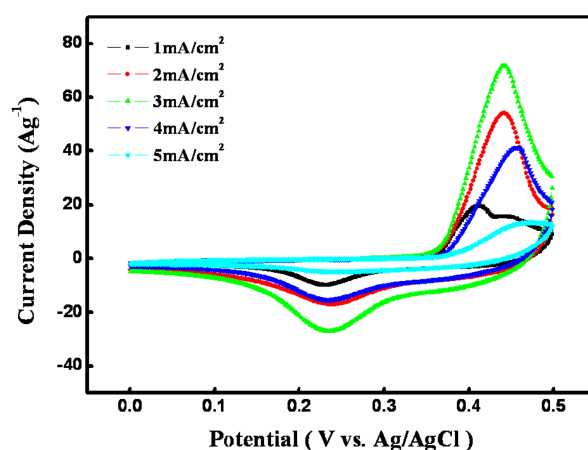
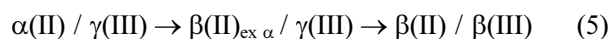


Fig. 5. Cyclic voltammograms(CV) of the Ni(OH)₂ electrodes prepared with different current densities.

the second cyclic voltammetry(CV) curves was to be 1233 Fg⁻¹. It was observed that the anodic peak potential shifts to a low potential with increasing cycles. At the same time, capacity was reduced as a whole. According to Ref. [30], the α-type material is first oxidized into γ(III) as similar inter-sheet distances characterize both α(II) and γ(III) phases. However, after one cycle, the discharged material shows the β(II) structural type. They have shown that the following sequence occurs during the several first electro-chemical cycles:



Therefore, as seen in Fig. 5, it is clear that the reduction of the anodic peak potential may be related to a phase conversion with increasing electrochemical cycles.

Cyclic voltammetry(CV) for the Ni(OH)₂ electrodes in 1 M KOH electrolyte, at a scan rate of 10 mVs⁻¹, are presented in Fig. 5. The shape of the curves shows that the capacitance characteristic was distinct from that of the electric double layer capacitor, which would produce a cyclic voltammetry(CV) curve that is usually close to an ideal rectangular shape. By overlapping the various cyclic voltammetry(CV) curves, it can be seen that the films at a 3 mA/cm² current density exhibit a cyclic voltammetry(CV) curve that encloses a greater area and thus these films have larger capacitance values. Gupta et al.(31) successfully synthesized α-Co(OH)₂ by potentiostatically depositing it onto a stainless-steel electrode from a 0.1 M Co(NO₃)₂ electrolyte at -1.0 V vs. Ag/AgCl. The specific capacitance of 860 F g⁻¹ was obtained for a 0.8 mg/cm² mass. Moreover, the deposited α-Co(OH)₂ showed very stable specific capacitance values even for a large deposited mass[31]. However, our results exhibit a drastic decrease at a high deposited mass.

Fig. 6 shows the dependence of specific capacitance on the deposited mass and current density in the Ni(OH)₂ films. The specific capacitance increases and peaks at 1233 F g⁻¹, when the current density increases and peaks at 3 mA/cm², and then decreases with

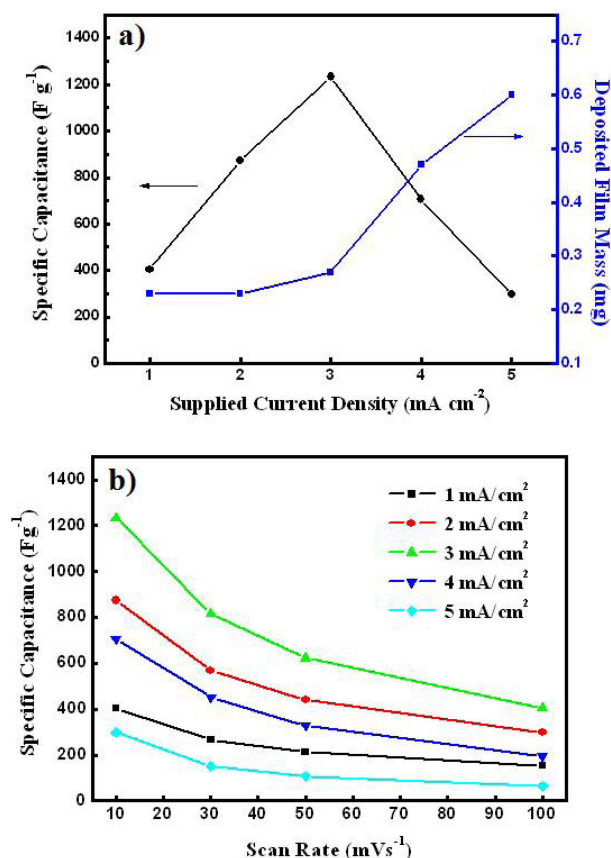


Fig. 6. (a) Plot of specific capacitance and deposited mass for Ni(OH)₂ films as a function of the current density. (b) Specific capacitance as a function of scan rate; for Ni(OH)₂ films galvanostatically deposited at different current densities.

increasing current density. The deposited weight increased with increasing current density for the electro-deposition of Ni(OH)₂ films. At a current density of 5 mA/cm², the weight increased to 0.6 mg while the specific capacitance decreased to 297 F g⁻¹. In general, capacitance increases with increasing current density, due to the deposited weight of the films. However, capacitance per unit weight decreased at current densities of 4 mA/cm², and 5 mA/cm². This could be considered to be due to the increase in weight of the Ni(OH)₂ films, and reduced surface area due to cracking (Fig. 7) This is in keeping

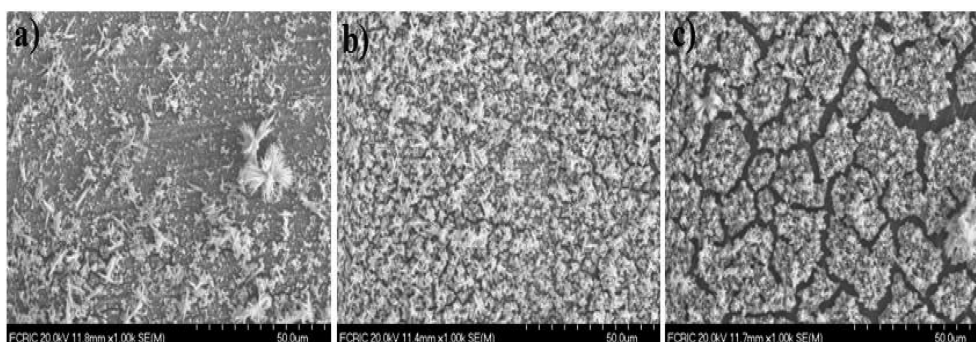


Fig. 7. Scanning electron microscope (SEM) images of Ni(OH)₂ electrodes prepared at different current densities after cyclic voltammetry tests: (a) 1 mA/cm², (b) 3 mA/cm², (c) 5 mA/cm².

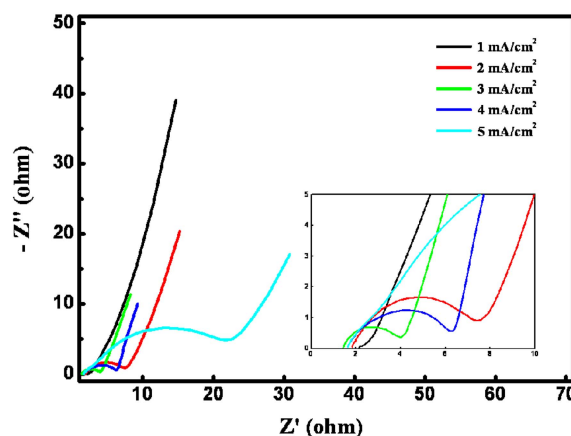


Fig. 8. The complex plane impedance plots of unit cells of the Ni(OH)₂ films prepared at different current densities.

with the work by Nagarajan et al. on a MnOx electrode prepared by potentiostatic deposition that behaved as an ideal capacitor within the window of 0-0.9 V [32]; but also found that the specific capacitance decreased with increasing sample weight. The specific capacitance measured at the scan rate of 20 mV s⁻¹ was found to be 328, 260 and 223 F g⁻¹ for deposited weights of 0.12, 0.18 and 0.30 mg/cm², respectively.

Fig. 7 shows the scanning electron microscope (SEM) images of Ni(OH)₂ electrodes, formed at various current densities, after testing by cyclic voltammetry. The morphology of each deposit is nano-structured with different surface morphologies. The deposited dimensions and cracks of the Ni(OH)₂ films vary depending on the current density which can lead to different capacitive behaviors. The nano-structured morphology of the Ni(OH)₂ films prepared at 3 mA/cm² possessed higher capacitance. However, the cracked morphology of the Ni(OH)₂ film prepared at 5 mA/cm² gave a relatively lower capacitance, as shown in Fig. 5.

The complex-plane impedance plots of unit cells of the Ni(OH)₂ films are shown in Fig. 8. The intercept at the real impedance (Z') axis of these plots indicates the combined series resistance of electrodes, electrolyte, and current collectors. The intercept for the Ni(OH)₂ film (prepared at 3 mA/cm²) is about 4, whereas this

value for the Ni(OH)₂ film (prepared at 5 mA/cm²) is over 20. The resistance of the Ni(OH)₂ film (prepared at 5 mA/cm²) was increased by the loss of adhesion of some active materials with the current collector or cracking during the galvanostatic deposition.

From the capacitance of the Ni(OH)₂ films (prepared at 3 mA/cm²) in 1 M KOH, it can be calculated that an energy density of about 21.4 Wh. kg⁻¹ and a power density of 3 kW. kg⁻¹ are attainable on a single cell device. Gupta et al. reported that, for an Al-substituted α -cobalt hydroxide, the specific energy density increased from 11.3 to 18.7 Whkg⁻¹ by the substitution of just 8 atomic percentage aluminum [33]. This indicates that the Ni(OH)₂ films are good and competitive candidates for the fabrication of pseudo-capacitors.

Conclusions

We have investigated supercapacitor electrodes based on Ni(OH)₂ films that were galvanostatically deposited onto stainless-steel substrates. The specific capacitance was found to depend on the weight and surface morphology of the Ni(OH)₂ films. As the current density increased, the deposited mass also increased but so did the impedance of the deposited film, because of the cracking of the deposited area. For the film prepared at a current density of 3 mA/cm², its specific capacitance was higher than the others and its impedance was lower. This indicates that the film manufactured at a current density of 3 mA/cm² may be more stable than the others. Wu et al. showed that a film deposited galvanostatically at a low current density of 0.25/cm² was more compact than at a high current density; especially near the surface of the substrate, and the film then becomes less compact further away from the surface of the substrate electrode [34]. Thus, due to the increase in connectivity and adhesion between particle/particle, and particle/substrate, the highest specific capacitance (1233 F g⁻¹) was obtained from the film prepared at a current density of 3 mA/cm².

Acknowledgement

This research was financially supported by the Ministry of Education, Science Technology (MEST), Gangwon Province, Gangneung City, Gangneung Science Industry Foundation (GSIF) as the R & D Project for Gangneung science park promoting program. Partially funding from New South Wales Government and the Australian Research Council is also gratefully acknowledged.

References

1. B.E. Conway, *Electrochemical Supercapacitors, Scientific Fundamentals and Technological Application*, Kluwer Academic/Plenum Press, New York (1999) 11.
2. S. Trasatti, and P. Kurzweil, *Platinum Met. Rev.* 38 (1994) 46-56.
3. S. Sarangapani, B.V. Tilak, and C.P. Chen, *J. Electrochem. Soc.* 143(1996) 3791-3799.
4. R.A. Huggins, *Solid State Ionics* 134 (2000) 179-195.
5. W. Sugimoto, H. Iwata, Y. Yasunaga, Y. Murakami, and Y. Takasu, *Angew.Chem. Int. Ed.* 42 (2003) 4092-4096.
6. W. Sugimoto, H. Iwata, Y. Yasunaga, Y. Murakami, and Y. Takasu, *J. Phys.Chem. B* 109 (2005) 7330-7338.
7. J.P. Zheng, P.J. Cygan, and T.R. Jow, *J. Electrochem. Soc.* 142 (1995) 2699-2703.
8. K.C. Liu; and M.A. Anderson, *J. Electrochem. Soc.* 143 (1996) 124-131.
9. E.E. Kalu; T.T. Nwoga; V. Srinivasan; and J.W. Weidner, *J. Power Sources* 92 (2001) 163-167.
10. C. Lin, J.A. Ritter, and B.N. Popov, *J. Electrochem. Soc.* 145 (1998) 4097-4103.
11. S.C. Pang, M.A. Anderson, and T.W. Chapman, *J. Electrochem. Soc.* 147 (2000) 444-450.
12. L. Cao, L.B. Kong, Y.Y. Liang, and H.L. Li, *Chem. Commun.* 14 (2004) 1646-1647.
13. L. Cao, F. Xu, Y.Y. Liang, and H.L. Li, *Adv.Mater.* 16 (2004) 1853-1857.
14. H. Bode, K. Dehmelt, and J. Witte, *Electrochim. Acta.* 11 (1966) 1079-1087.
15. T.N. Ramesh, R.S. Jayashree, P.V. Kamath, S. Rodrigues, and A.K. Shukla, *J. Power Sources* 104 (2002) 295-298.
16. W.K. Hu, and D. Noreus, *Chem. Mater.* 15 (2003) 974-978.
17. Z. Chang, H. Tang, and J.G. Chen, *Electrochem. Commun.* 1 (1999) 513-516.
18. D.D. Zhao, W.J. Zhou, and H.L. Li, *Chem. Mater.* 19 (2007) 3882-3891.
19. M.S. Wu, and H.H. Hsieh, *Electrochim. Acta.* 53 (2008) 3427-3435.
20. Q.H. Huang, X.Y. Wang, J. Li, C.L. Dai, S. Gamboa, and P. J. Sebastian, *J. Power Sources* 164 (2007) 425-429.
21. G.S. Attard, P.N. Bartlett, N.R.B. Coleman, J.M. Elliott, J. R. Owen, and J.H. Wang, *Science* 278 (1997) 838-840.
22. P.A. Nelson, J.M. Elliott, G.S. Attard, and J.R. Owen, *Chem.Mater.* 14 (2002) 524-529.
23. Y. Tan, S. Srinivasan, and K.S. Choi, *J. Am. Chem. Soc.* 127 (2005) 3596-3599.
24. D.A. Corrigan, and R.M. Bendert, *J. Electrochem. Soc.* 136 (1989) 723-727.
25. C.F. Baes, and R.E. Mesmer, in *The Hydrolysis of Cations*, John Wiley & Sons: New York (1976) 489.
26. C.C. Streinz, S. Motupally, and J.W. Weidner, *J. Electrochem. Soc.* 142 (1995) 4051-4056.
27. P.V. Kamath, M. Dixit, L. Indira, A.K. Shukla, V.G. Kumar, and N. Munichandraiah, *J. Electrochem. Soc.* 141 (1994) 2956-2959.
28. J. Jiang, and A. Kucernak, *Chem. Mater.* 16 (2004) 1362-1367.
29. C. Natarajan, H. Matsumoto, and G. Nogami, *J. Electrochem. Soc.* 144 (1997) 121-126.
30. A. Delahaye-Vidal, B. Beaudoin, N. Sac-Epee, K. Tekaiia-Elhsissen, A. Audemer, and M.
31. Figlarz, *Solid State Ionics* 84 (1996) 239-244.
32. V. Gupta, T. Kusahara, H. Toyama, S. Gupta, and N. Miura, *Electrochem. Commun.* 9 (2007) 2315-2319.
33. N. Nagarajan, H. Humadi, and I. Zhitomirsky, *Electrochim. Acta.* 51 (2006) 3039-3045.
34. V. Gupta, S. Gupta, and N. Miura, *J.Power Sources* 177 (2008) 685-689.
35. M.S. Wu, C.H. Yang, and M.J. Wang, *Electrochim. Acta.* 54 (2008) 155-161.